ChemComm

COMMUNICATION

View Article Online
View Journal

Cite this: DOI: 10.1039/c6cc07825g

Received 26th September 2016,
Accepted 14th November 2016

DOI: 10.1039/c6cc07825g

www.rsc.org/chemcomm

Highly efficient three-component coupling reaction catalysed by atomically precise ligand-protected $Au_{38}(SC_2H_4Ph)_{24}$ nanoclusters†

Qi Li, Anindita Das,‡ Shuxin Wang, Yuxiang Chen and Rongchao Jin*

The catalytic potential of atomically precise quantum-sized gold nanoclusters ($Au_{38}(SC_2H_4Ph)_{24}$) is explored for the three-component coupling of an aldehyde, an alkyne and an amine to synthesize propargylamines. A high catalytic efficiency with a very low loading (0.01 mol%) is achieved. Furthermore, the synergistic effect of the electron-deficient surface (*i.e.* $Au^{\delta+}$, $0 < \delta^+ < 1$) and the electron-rich Au_{23} core of the ligand-protected nanoclusters is critical for this catalytic reaction.

Metal nanoparticles (1–100 nm) occupy an important position in heterogeneous catalysis.[1,2] The high activity of small particles arises from their high surface area-to-volume ratio, surface geometric effect, electronic properties, and quantum size effect.[3–6] However, the elusive surface structure of nanoparticles poses a major challenge to correlating the catalytic performance with the catalyst structure.[1–6] In recent research, atomically precise gold nanoclusters (<2 nm) protected by thiolate ligands have emerged as a new class of nanocatalysts, which have been reported to exhibit good catalytic performance for a range of reactions.[7–15] Compared to conventional gold nanocatalysts (for example, larger nanoparticles), whose surface structures are unknown, atomically precise gold nanoclusters possess well-defined atomic structures, so that they can serve as model nanocatalysts for investigating how the atomic structure and the catalytic properties are related.

Three-component coupling of an aldehyde, an alkyne and an amine (generally called A^3 coupling) is the most convenient and general approach to synthesize propargylamines, which are well-recognized as highly valuable synthetic building blocks in the synthesis of various natural products and biologically active compounds.[16] To date, many transition-metal catalysts including gold,[17] silver,[18] copper,[19] iridium,[20] nickel,[21] iron,[22] and indium[23] have been explored for the synthesis of propargylamines. Among them, gold catalysts, especially Au(III) salts, show the highest catalytic efficiency. For example, in 2003 Wei *et al.*[17] first demonstrated that both Au(III) and Au(I) salts can be used as highly efficient catalysts for the A^3 coupling reaction, with a TOF up to $\sim 34\ h^{-1}$ for Au(III) salts and $\sim 8.3\ h^{-1}$ for Au(I) salts at 99% conversion. However, the shortcomings of typical homogeneous catalysis are multi-fold, such as the difficulty in separation, poor recyclability and thermal instability. Gold nanoparticles can overcome such shortcomings. In 2007, Kidwai[24] *et al.* first reported that the A^3 coupling reaction could be readily accomplished by using unsupported-Au(0) nanoparticles, although the efficiency was very low. Several critical issues still remain for gold nanoparticles to be used as the catalyst for A^3 coupling. First, to date, only those nanogold catalysts supported on some specially designed supports which are usually laborious and time-consuming to prepare (such as montmorillonite, magnesium oxide, mesoporous carbon nitride, mesoporous organosilica with ionic liquid frameworks)[25–28] have shown enhanced catalytic performance (TOFs: 10–40 h^{-1}). More importantly, the active site of gold nanoparticle catalysts remains elusive. This is due to several factors, including the unknown surface structure of the gold nanoparticles, the complicated unknown effect of different supports and also the probable residual Au(III) salt precursor on the support that may significantly impact the reaction.

Herein, atomically precise and thermally stable $Au_{38}(SC_2H_4Ph)_{24}$ nanoclusters are explored as a catalyst for the A^3 coupling reaction. The atomic structure of the $Au_{38}(SC_2H_4Ph)_{24}$ nanocluster was previously determined by X-ray crystallography,[29] which is composed of a face-fused biicosahedral core (Au_{23}) protected by six dimeric $Au_2(SR)_3$ and three monomeric $Au(SR)_2$ staple-like surface motifs (Fig. 1). This enables a detailed analysis of the relation between the cluster structure and the catalytic performance, which couldn't be realized in previous research on larger gold nanoparticles. We hypothesize that the electron-rich Au_{23} core and the surface shell of Au atoms carrying partial positive charges ($0 < \delta^+ < 1$) on account of bonding to thiolates in the staple motifs (Fig. 1b) may synergistically boost the catalytic performance. Furthermore, ligand-off Au_{38} clusters with the Au(0)

Department of Chemistry, Carnegie Mellon University, Pittsburgh, PA 15213, USA. E-mail: rongchao@andrew.cmu.edu

† Electronic supplementary information (ESI) available. See DOI: 10.1039/c6cc07825g

‡ Current address: Department of Chemistry, Northwestern University, Evanston IL 60208, USA.

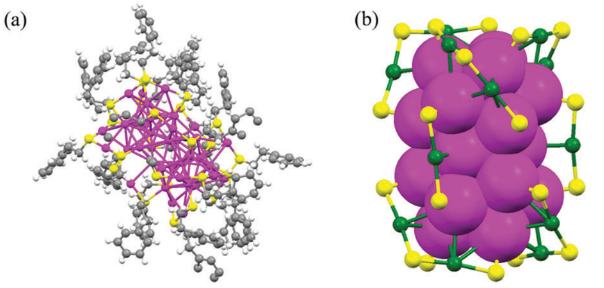

Fig. 1 (a) The X-ray crystal structure of the $Au_{38}(SC_2H_4Ph)_{24}$ cluster. Magenta is Au, yellow is sulfur, gray is carbon and white is hydrogen. (b) The core/shell structure of the cluster: a face-fused biicosahedral Au_{23} core protected by six dimeric $Au_2(SR)_3$ and three monomeric $Au(SR)_2$ staple-like surface motifs (carbon and hydrogen are omitted); Au atoms in the motifs (green) carry partial positive charges ($0 < \delta^+ < 1$) due to bonding with thiolate ligands.

surface can also be easily obtained after thermal pretreatment (*e.g.* at 300 °C in N_2 for 1 hour), which provides an exclusive comparison of the catalytic behavior of Au(0) and $Au^{\delta+}$ ($0 < \delta^+ < 1$) surface sites on nanogold.

The three-component coupling reaction of an aldehyde, an alkyne and an amine is shown in Fig. 2a. In this work, catalytic tests indicate that the $Au_{38}(SC_2H_4Ph)_{24}$ clusters are highly efficient catalysts for the A^3-coupling reaction. An excellent conversion up to 98% to the propargylamine product can be achieved in 5 h (indicated by NMR analysis, see Fig. S1, ESI†). The reaction kinetics was studied by monitoring the conversion of reactants at different time intervals, as shown in Fig. 2b. It was found that the conversion to propargylamine increased rapidly during the first few hours, reaching a maximum (>90%) within 4 h and higher for a prolonged period of time. The kinetics can be well fitted by a first-order equation (Fig. 2c) and the reaction rate constant is calculated to be $k = 0.6\ h^{-1}$. The turnover frequencies (TOFs) at 2.4% conversion after initial 6 min run are calculated to be 2465 h^{-1} per Au_{38} cluster and 65 h^{-1} per gold atom. After 5 hours, the reaction reached the maximum conversion (98%); the calculated turnover numbers (TONs) per Au_{38} cluster and per gold atom are 9800 and 258, respectively.

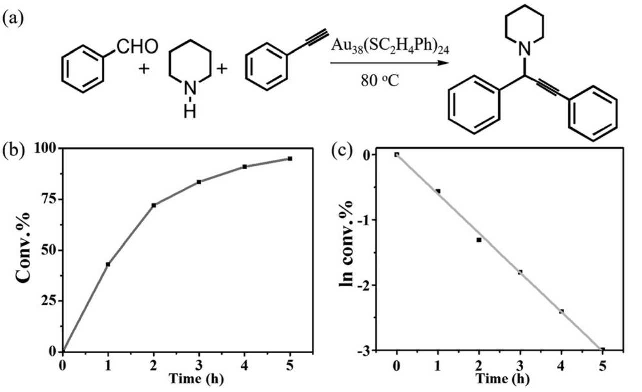

Fig. 2 (a) Scheme of three-component coupling reaction of benzaldehyde, piperidine, and phenylacetylene for the synthesis of propargylamine catalyzed by $Au_{38}(SC_2H_4Ph)_{24}$. (b) Conversion of benzaldehyde, phenylacetylene and piperidine as a function of reaction time over $Au_{38}(SC_2H_4Ph)_{24}$ catalysts. (c) Linear relation between the natural logarithm of conversion and time. Reaction conditions: benzaldehyde (1.0 mmol), piperidine (1.2 mmol), and phenylacetylene (1.3 mmol), 80 °C. $Au_{38}(SC_2H_4Ph)_{24}$: 1 mg (0.1×10^{-3} mmol, 0.01 mol% loading).

We further characterized the $Au_{38}(SC_2H_4Ph)_{24}$ catalyst after the A^3 coupling reaction by UV-visible spectroscopy (Fig. S2, ESI†) and ESI-mass spectrometry (Fig. S3, ESI†). The optical peaks of the $Au_{38}(SC_2H_4Ph)_{24}$ cluster at 450 nm, 630 nm and 750 nm are retained, indicating that the majority of the $Au_{38}(SC_2H_4Ph)_{24}$ clusters survived the reaction. This was further confirmed by the ESI-mass spectrometric analysis of the $Au_{38}(SC_2H_4Ph)_{24}$ catalyst after the reaction, which shows peaks corresponding to the $Au_{38}(SC_2H_4Ph)_{24}$ clusters.

The recyclability of the catalyst is also of high importance for real-world applications, and we investigated this by recycling the catalyst (*i.e.* adding excess methanol to precipitate clusters) for reuse in fresh reactions. With the recycled catalyst, a fresh reaction was performed with fresh reactants under identical reaction conditions. It was observed that the conversion was decreased from 98% to ~68% after 3 cycles. The drop in conversion should be caused by the gradual degradation of nanoclusters in the multiple recycling tests. Overall, the gold nanocluster catalysts show a reasonably good recyclability.

It should be noted that the $Au_{38}(SC_2H_4Ph)_{24}$ cluster, with a well-defined structure, comprising an Au(0) core protected by $Au^{\delta+}$–thiolate ($0 < \delta^+ < 1$) motifs, shows a much higher catalytic efficiency for the A^3 coupling reaction than any other larger gold(0) nanoparticles and Au(I) salt/complex based catalysts reported before. We rationalize that the electronic structure of the $Au_{38}(SC_2H_4Ph)_{24}$ nanocluster, including the surface ligand protected partially charged $Au^{\delta+}$ atoms and the electron-rich Au_{23} core, is critical for this significant enhancement of catalytic efficiency. To further verify this, another nanocluster with an atomically well-defined structure, $Au_{25}(SC_2H_4Ph)_{18}^-$ (composed of an icosahedral core Au_{13} and six $Au_2(SR)_3$ staple motifs),[7,30] was also tested as the catalyst for the A^3 coupling reaction. The experimental results demonstrate that the $Au_{25}(SC_2H_4Ph)_{18}^-$ cluster shows a similarly high catalytic performance to $Au_{38}(SC_2H_4Ph)_{24}$. The kinetics and product conversion of A^3 reaction catalyzed by $Au_{25}(SC_2H_4Ph)_{18}^-$ are similar to the Au_{38} catalyzed case (shown in Fig. S4, ESI†), which agrees well with our rationale.

We also investigated the $Au_{38}(SC_2H_4Ph)_{24}$ nanocluster supported on different metal-oxides, including cerium dioxide (CeO_2), titanium dioxide (TiO_2), and silica (SiO_2), for the A^3 coupling. As shown in Table 1, $Au_{38}(SC_2H_4Ph)_{24}$ clusters loaded on all the different supports show similarly high catalytic performance to the unsupported one. These results are totally different from previously reported larger gold nanoparticle catalysts, in which high catalytic performance can be achieved only by loading gold nanoparticles on specially designed oxide supports.[25–28] Our results suggest that the intrinsic electronic structure of the ligand-protected nanoclusters plays a determinant role in their catalytic performance, as opposed to the case of bare nanogold on special supports.

To gain further insight into the relation between the cluster structure and the catalytic performance, ligand-off Au_{38} clusters supported on CeO_2 were prepared through a thermal method

Table 1 Three-component coupling of benzaldehyde, piperidine, and phenylacetylene with the $Au_{38}(SC_2H_4Ph)_{24}$ cluster catalyst loaded on different supports in different solvents[a]

Catalyst	Solvent	T (°C)	Time (h)	Conv. (%)
Au_{38}	No solvent	80	5	98
Au_{38}/TiO_2	No solvent	80	5	93
Au_{38}/SiO_2	No solvent	80	5	98
Au_{38}/CeO_2	No solvent	80	5	99
Au_{38}/CeO_2	Water	80	5	94
Au_{38}/CeO_2	Toluene	80	5	80

[a] Reaction conditions: benzaldehyde (1.0 mmol), piperidine (1.2 mmol), and phenylacetylene (1.3 mmol), 1 mg of $Au_{38}(SC_2H_4Ph)_{24}$ supported by 100 mg of metal oxides, 1 mL of H_2O (MilliQ) or toluene if needed, 5 h, 80 °C.

reported previously.[31,32] After thermal pretreatment under 300 °C in N_2, all the ligands can be removed, leaving exposed Au(0) atoms on the cluster surface. The catalytic performance of the ligand-off Au_{38}/CeO_2 was, however, found to be significantly decreased (Fig. 3) compared with the ligand-on $Au_{38}(SC_2H_4Ph)_{24}$ nanoclusters. This is against the traditional view that more bare surface atoms would lead to higher catalytic performance. The conversion to the product decreases from $>95\%$ to 70% after a 5 h-run and no more product can be obtained upon prolonging the time. More importantly, the reaction kinetics change from first-order to nearly zero-order when ligand-off Au_{38}/CeO_2 was used as the catalyst, suggesting that the underlying reaction pathway may have been changed.

For comparison, an Au(I)–S–C_2H_4Ph complex was also prepared and its catalytic performance for the A^3 coupling was tested. The results show that the final conversion significantly decreases to 60% (note: for Au(I)–S–C_2H_4Ph, an equivalent mole of gold as the $Au^{\delta+}$–thiolate on the $Au_{38}(SC_2H_4Ph)_{24}$ is used as the catalyst under the same reaction conditions).

The above results further demonstrate the importance of the intact structure of $Au_{38}(SC_2H_4Ph)_{24}$ for the catalytic performance. Both the $Au^{\delta+}$–thiolate surface and the electron rich Au(0) core are important and the synergistic effect of the core and the shell results in an enhanced catalytic performance.

To test the scope of the A^3 coupling reaction with the $Au_{38}(SC_2H_4Ph)_{24}$ clusters, we extended our studies to different combinations of aldehydes and alkynes. As shown in Table 2, different benzaldehydes give excellent yields in the A^3 coupling reactions (entries 1–7), except for the one with 4-nitrobenzaldehyde, which contains a strongly electron-withdrawing group (entry 7). On the other hand, different alkynes show distinctly different yields. The phenylacetylene derivatives show similarly high conversions (entries 8 and 9) under the same reaction conditions, but other alkynes display decreasing yields (entries 10 and 11).

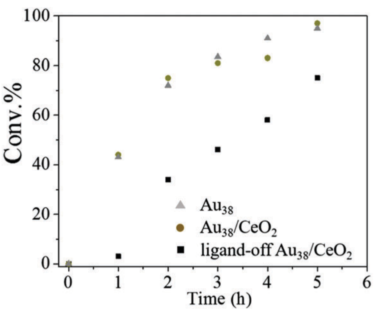

Fig. 3 Conversion of benzaldehyde, phenylacetylene and piperidine as a function of reaction time over $Au_{38}(SC_2H_4Ph)_{24}$, $Au_{38}(SC_2H_4Ph)_{24}/CeO_2$, and ligand-off Au_{38}/CeO_2 catalysts.

Table 2 A^3 coupling of an aldehyde, alkyne, and amine catalyzed by $Au_{38}(SC_2H_4Ph)_{24}$[a]

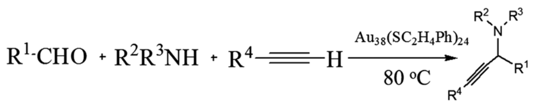

Entry	R^1	R^2R^3NH	R^4	Time (h)	Yield [%]
1	Ph	Piperidine	Ph	5	95
2	p-Br-Ph	Piperidine	Ph	5	91
3	p-CH_3S-Ph	Piperidine	Ph	5	91
4	p-CH_3-Ph	Piperidine	Ph	5	84
5	p-F-Ph	Piperidine	Ph	5	93
6	p-CH_3O-Ph	Piperidine	Ph	5	92
7	p-NO_2-Ph	Piperidine	Ph	5	0
8	Ph	Piperidine	o-CH_3-Ph	5	90
9	Ph	Piperidine	p-CH_3O-Ph	5	100
10	Ph	Piperidine	Ph-$(CH_2)_2$	5	62
11	Ph	Piperidine	$CH_3(CH_2)_5$	5	31

[a] Reaction conditions: aldehyde (1 equiv., 1.0 mmol), amine (1.2 equiv., 1.2 mmol), alkyne (1.3 equiv., 1.3 mmol), 0.01 mol% $Au_{38}(SC_2H_4Ph)_{24}$ catalyst.

The mechanism of the A^3 coupling reaction has not been well-explored in the literature.[16] A general reaction pathway involves C–H activation of the alkyne, forming an intermediate π-metal–alkyne complex, which then reacts with the iminium ion, resulting in the formation of propargylamine with simultaneous regeneration of the metal catalyst. It has been demonstrated that phenylacetylene can be facially absorbed on the Au cluster surface, with its phenyl ring facing an external gold atom of the cluster which is well exposed with little steric hindrance.[9] Meanwhile, previous work also demonstrated the various strong bonding modes of phenylacetylene on the surface of gold nanoclusters.[33] This is consistent with our experimental results that alkynes (*i.e.* the lack of a phenyl ring and hence weaker adsorption) show significantly decreased yields compared with the phenylacetylene derivatives (Table 2, entries 8–11). Our results also suggest that the benzaldehydes have strong adsorption energy with the –CHO group in close contact with the S–Au–S groups.[34] As the –NO_2 group can also interact with the S–Au–S motif, which can influence the orientation of NO_2–Ph–CHO on the cluster surface,[34] this explains the result of NO_2–Ph–CHO undergoing no conversion to propargylamines. We performed NMR measurements for the Au_{38} cluster after running the A^3 reaction and being washed with ethanol for many times, but no trace of phenylacetylene and benzaldehydes could be found; this may arise from the relatively weak interaction of the Au cluster with phenylacetylene and benzaldehydes, so that they are easily washed away in the isolation steps of the clusters from the reaction mixture.

In summary, we have explored the $Au_{38}(SC_2H_4Ph)_{24}$ nanocluster as a catalyst for multi-component A^3 coupling reaction.

The $Au_{38}(SC_2H_4Ph)_{24}$ nanocluster is found to catalyze the A^3 reaction with a very high efficiency. We further demonstrate the importance of the entire structure of the $Au_{38}(SC_2H_4Ph)_{24}$ cluster, *i.e.* the synergistic effect of the ligand protected $Au^{\delta+}$ surface ($0 < \delta^+ < 1$) and the electron-rich Au_{23} core for high catalytic performance. Such nanocluster catalysts may find promising application in other transformation reactions and provide mechanistic insights.

R. J. acknowledges the financial support from the U.S. National Science Foundation (DMREF-0903225).

Notes and references

1 J. M. Thomas and W. Thomas, *Principles and Practices of Heterogeneous Catalysis*, Wiley, New York, 1996.
2 G. C. Bond, C. Louis and D. T. Thompson, *Catalysis by Gold*, Imperial College Press, London, 2006.
3 R. Jin, *Nanotechnol. Rev.*, 2012, **1**, 31.
4 Y. Isomura, T. Narushima, H. Kawasaki, T. Yonezawa and Y. Obora, *Chem. Commun.*, 2012, **48**, 3784.
5 Y. Song, J. Zhong, S. Yang, S. Wang, T. Cao, J. Zhang, P. Li, D. Hu, Y. Pei and M. Zhu, *Nanoscale*, 2014, **6**, 13977.
6 G. A. Somorjai, R. L. York, D. Butcher and J. Y. Park, *Phys. Chem. Chem. Phys.*, 2007, **9**, 3500.
7 G. Li and R. Jin, *Acc. Chem. Res.*, 2013, **46**, 1749.
8 T. Higaki, H. Kitazawa, S. Yamazoe and T. Tsukuda, *Nanoscale*, 2016, **8**, 11371.
9 G. Li, D. Jiang, C. Liu, C. Yu and R. Jin, *J. Catal.*, 2013, **306**, 177.
10 M. B. Li, S. K. Tian and Z. Wu, *Nanoscale*, 2014, **6**, 5714.
11 M. Boronat, A. Leyva-perez and A. Corma, *Acc. Chem. Res.*, 2014, **47**, 834.
12 J. Liu, K. S. Krishna, Y. B. Losovyj, S. Chattopadhyay, N. Lozova, J. T. Miller, J. J. Spivey and C. S. S. R. Kumar, *Chem. – Eur. J.*, 2013, **19**, 10201.
13 A. Shivhare, S. J. Ambrose, H. Zhang, R. W. Purves and R. W. J. Scott, *Chem. Commun.*, 2013, **49**, 276.
14 G. Li and R. Jin, *J. Am. Chem. Soc.*, 2014, **136**, 11347.
15 G. Li, C. Liu and R. Jin, *Chem. Commun.*, 2012, **48**, 12005.
16 V. Peshkov, O. Pereshivko and E. Eycken, *Chem. Soc. Rev.*, 2012, **41**, 3790.
17 C. Wei and C. J. Li, *J. Am. Chem. Soc.*, 2003, **125**, 9584.
18 C. Wei, Z. Li and C. J. Li, *Org. Lett.*, 2003, **5**, 4473.
19 S. Nakamura, M. Ohara, Y. Nakamura, N. Shibata and T. Toru, *Chem. – Eur. J.*, 2010, **16**, 2360.
20 S. Sakaguchi, T. Kubo and Y. Ishii, *Angew. Chem., Int. Ed.*, 2001, **40**, 2534.
21 K. Namitharan and K. Pitchumani, *Eur. J. Org. Chem.*, 2010, 411.
22 T. Zeng, W.-W. Chen, C. M. Cirtiu, A. Moores, G. Song and C.-J. Li, *Green Chem.*, 2010, **12**, 570.
23 Y. Zhang, P. Li, M. Wang and L. Wang, *J. Org. Chem.*, 2009, **74**, 4364.
24 M. Kidwai, V. Bansal, A. Kumar and S. Mozumdar, *Green Chem.*, 2007, **9**, 742.
25 K. Layek, R. Chakravarti, M. Lakshmi Kantam, H. Maheswaran and A. Vinu, *Green Chem.*, 2011, **13**, 2878.
26 K. K. R. Datta, B. V. S. Reddy, K. Ariga and A. Vinu, *Angew. Chem., Int. Ed.*, 2010, **49**, 5961.
27 B. Karimi, M. Gholinejad and M. Khorasani, *Chem. Commun.*, 2012, **48**, 8961.
28 B. Borah, S. Borah, K. Saikia and D. Dutta, *Catal. Sci. Technol.*, 2014, **4**, 4001.
29 H. Qian, W. T. Eckenhoff, Y. Zhu, T. Pintauer and R. Jin, *J. Am. Chem. Soc.*, 2010, **132**, 8280.
30 M. Zhu, E. Lanni, N. Garg, M. E. Bier and R. Jin, *J. Am. Chem. Soc.*, 2008, **130**, 1138.
31 X. Nie, H. Qian, Q. Ge, H. Xu and R. Jin, *ACS Nano*, 2012, **6**, 2014.
32 X. Nie, C. Zeng, X. Ma, H. Qian, Q. Ge, H. Xua and R. Jin, *Nanoscale*, 2013, **5**, 5912.
33 X. Wan, W. Xu, S. Yuan, Y. Gao, X. Zeng and Q. Wang, *Angew. Chem., Int. Ed.*, 2015, **127**, 9819.
34 G. Li, D. Jiang, S. Kumar, Y. Chen and R. Jin, *ACS Catal.*, 2014, **4**, 2463.